Tumor detection by simultaneous bilateral diffuse optical tomography (DOT) breast imaging

Yaling Pei[1], Harry L. Graber[1,2], Mark Farber[2], Christoph H. Schmitz[1,3], Yong Xu[1,2], Paul Toubas[2], Naresh Patel[2], Michael S. Katz[4], William B. Solomon[2], and Randall L. Barbour[1,2]

[1]NIRx Medical Technologies LLC; [2]SUNY Downstate Medical Center; [3]Charité—Universitätsmedizin Berlin; [4]SUNY Buffalo School of Medicine

Background & Introduction

- Dynamic Near Infrared Optical Tomography (DYNOT)
  - Provides measures of relative concentrations of hemoglobin (Hb)
    - Oxygenated, deoxygenated, total
  - Noninvasive functional imaging *in vivo*
    - Exogenous contrast agents not required
- Growth of solid tumors frequently accompanied by:
  - Marked changes in the vascular supply sustaining tumor growth [1]
    - State of impaired perfusion
    - Relatively hypoxic environment
- To image the preceding features, we developed:
  - Dual-breast DOT imaging system
  - Capable of simultaneous bilateral measurements

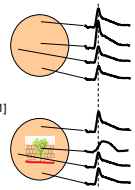

- Healthy Breast
  - Coherent response to provocation
- Tumor Breast
  - Sluggish perfusion
  - Reduced response to natural effectors
  - Elevated Hb levels

DYNOT Imager

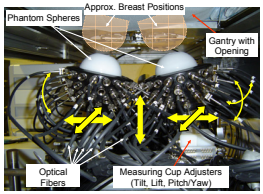

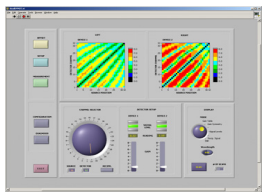

- (Left) DYNOT simultaneous dual-breast measuring head [2]
  - Data collected from 124 channels (62 fibers × 2 wavelengths) in parallel
  - Sources location is time-multiplexed
  - Measurement rate: 2 complete image frames (> 3×10^4 data points) per second
- (Right) GUI for imager control
  - Allows real-time viewing of data as they are collected
  - Automated process for determining appropriate amplification (gain) factors for all data channels
  - Extensive capabilities for:
    - Pre-measurement system checks
    - Testing fidelity of fiber-skin contact

Dynamic Phantom Studies

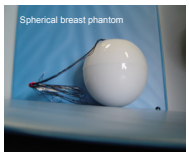

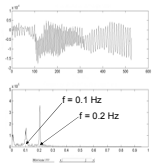

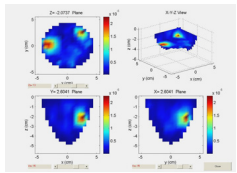

- (Left) Laboratory phantom medium
  - Approximates size and shape of a breast
  - Has defined background optical coefficient values
  - Contains a pair of electrochromic devices
    - Independently controllable
    - Absorption coefficient (μ_a) can be changed by adjusting the applied voltage
    - Can be programmed to produce a pre-selected μ_a time series.
- Experimental test shows that DYNOT imager:
  - (Middle) Detects the programmed signals with high temporal fidelity
  - (Right) Accurately localizes an idealized lesion inside the medium

Physiological Insight → Clinical Study Design

- Well-characterized differences between vasculature in healthy tissue (or in non-cancer pathologies), and in cancerous solid tumors [1]
  - Mechanisms exist, by which a cancerous tumor's "volume of influence" may be appreciably larger than the tumor itself [1,3]
- A key to increasing diagnostic power is comparing detector and image data between the two simultaneously examined breasts
  - Vascular responses under autonomic control should be similar in the two breasts
  - Responses under autoregulatory (local) control also should be similar, if both breasts are healthy
- If one breast has a cancerous tumor and the other doesn't, what macroscopic differences could we expect?
  - Increased amplitudes for vasomotor rhythms, in the tumor-bearing breast (TBB)
    - Owing to hypoxic environment of many solid tumors
  - Greater degree of temporal coordination, and greater spatial homogeneity, in the tumor-free breast (TFB)
  - Abnormal response, in the TBB, to events that stress the microvasculature
- Three categories of diagnostic metrics are considered
  - Each is devised to reveal one of the three previously outlined types of expected difference between the TBB and TFB
  - **Group 1:** Indices of resting vasomotion amplitude
    - Computed from baseline (*i.e.*, subject at rest) measurement data
    - Are sensitive to enhanced vasomotion
  - **Group 2:** Index of spatially coordinated dynamics
    - Computed from baseline measurement data
    - Is sensitive to differences in timing of blood delivery, between the two breasts

Physiological Insight → Clinical Study Design (cont.)

- Three categories of diagnostic metrics (cont.)
  - **Group 3:** Measures of pressure-induced blood volume and oxygenation shifts
    - Computed from data collected during Valsalva maneuver
    - Are sensitive to venous congestion and delayed reperfusion
    - In the TBB, relative to the contralateral TFB, one would expect to see:
      - Increased oxygen desaturation of Hb
      - Increased blood volume change
      - Time-lagged responses
- Essential strategy for image time series analysis: Figure 1
- Differences between metric values, for each subject's two breasts, are calculated as:
  - Tumor minus non-tumor for training-set cancer subjects
  - Left minus right for training-set non-cancer subjects, and for validation-set subjects
- Each metric is converted into six candidate diagnostic parameters, by normalizing the inter-breast difference in a variety of ways:
  - Difference divided by larger, smaller, or average value of the two individual-breast values
  - Difference multiplied by larger, smaller, or average of the individual-breast values
- Assessment of sensitivity (SN), specificity (SP), positive and negative predictive values (PPV, NPV)
  - Univariate: unequal-variance t-test for difference between means of CA and non-CA subgroups of the training set
    - Spot-check with non-parametric Mann-Whitney test, to ensure that small sample sizes is not an issue
  - Multivariate: logistic regression (LR)
    - Initial model is a linear combination of all univariate predictors that yield statistically significant differences between the sub-group means
    - Use a LR algorithm to find the optimal coefficients for the model
    - Remove redundant metrics (i.e., eliminate least significant metric from the model and repeat LR computation)
    - Use leave-out-one cross-validation (LOOCV) to determine sensitivity to idiosyncrasies of the training-set subjects

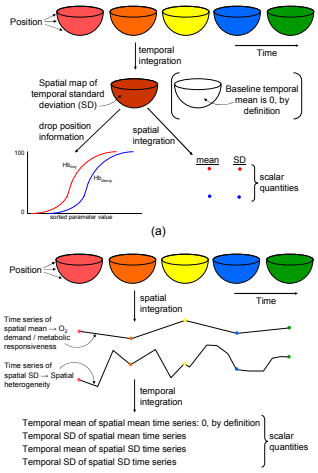

Figure 1. Schematics of the processing steps used to distill all the information in a 4D image time series into scalar diagnostic metrics. (a) Integrate over the spatial dimensions, then compute temporal descriptive statistics; (b) Spatial and temporal dimensions considered in the opposite order.

Clinical Study Results

- Patient population: 37 volunteers
  - 14 with breast cancer and 23 healthy controls
    - Groups are matched in terms of age and body-mass index
    - Heterogeneous control group: includes healthy subjects and subjects having non-cancer breast pathologies
  - Data are processed [4,5] to produce time series of volumetric images for each Hb state parameter: HbOxy, HbDeoxy, HbTotal, and HbO_2 Sat
- Univariate Analysis
  - SN, SP, PPV, NPV ranges (minimum, maximum, mean) are summarized in Table 1
    - Range includes *all* univariate metrics
      - Whether or not they show a statistically significant sub-group mean difference
  - For the metrics that *are* statistically significant predictors, predictive values range from 57% to 91%
  - Mean predictive values range from 60% to 86%, when each Metric Group is considered separately
  - Taking all Metric Groups collectively, mean PPV is 69% and mean NPV is 81%
- Multivariate Analysis
  - SN, SP, PPV, NPV ranges (minimum, maximum, mean) are summarized in Table 2
    - Predictive models including Group 3 metrics can consider only 21 subjects
    - Models including only Group 1 and/or 2 metrics include all 37 subjects
  - Composite clinical predictive values can increase markedly, relative to the constituent univariate predictors (UPs)
    - Range is from 82% to 100%
    - Best-case composite having minimum values >90% for each of SN, SP, PPV, and NPV
- Validation Study
  - Compute values UPs, for the subjects in the validation set
  - Combine new UP values with multivariate-predictor coefficients derived from the training-set subjects
    - Compute a probability of CA for each validation-set subject (Figure 2)

Table 1. Diagnostic Measures for Group 1 - 3 Data Minimum – Maximum (Mean)

	Sensitivity	Specificity	PPV	NPV
Composite Group 1 Data	50.0-85.7(72.5)	56.5-84.2(72.7)	50.0-78.6(62.0)	70.8-90.0(81.5)
Composite Group 2 Data	42.9-78.6 (59.8)	56.5-95.7 (82.6)	44.4-88.9 (69.8)	68.4-82.4 (77.1)
Composite Group 3 Data	70.0-90.0 (83.3)	72.7-100 (86.4)	75.0-100 (85.7)	76.9-91.7 (85.2)
Average Composite For Groups 1-3	42.9-90.0 (70.7)	56.5-100 (78.6)	44.4-100 (69.0)	68.4-91.7 (80.7)

Table 2. Summary of Multivariate Analysis Results

Formulation	$N_{subjects}$	$N_{metrics}$	Hb States Included	Data Groups Included	Sens. (%)	Spec. (%)	PPV (%)	NPV (%)	
Diff./Max.	21	3	Oxy (2), Total (1)	1, 3	100	90.9	90.1	100	All Subjects
					87.5	90.0	87.5	90.0	LOOCV
Diff.*Max	21	3	Oxy (1), Deoxy (1), Total (1)	1, 2, 3	100	81.8	83.3	100	All Subjects
					70.0	90.0	87.5	75.0	LOOCV
Diff.*Max.	37	5	Oxy (3), Deoxy (1), Total (1)	1, 2	100	87.0	82.4	100	All Subjects
					85.7	73.9	66.7	89.5	LOOCV

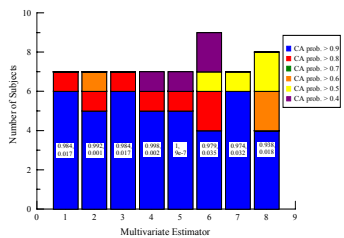

Figure 2. Probability of disease for indicated number of subjects, for eight different multivariate estimators. Inset in bar graph is the mean and SD probability for the >90% decile.

References

[1] M. Molls and P. Vaupel (Eds.), *Blood Perfusion and Microenvironment of Human Tumors: Implications for Clinical Radiooncology* (Springer-Verlag, Berlin, 2000).

[2] C.H. Schmitz, H.L. Graber, Y. Pei, M.B. Farber, M. Stewart, R.D. Levina, M.B. Levin, Y. Xu, and R.L. Barbour, "Dynamic studies of small animals with a four-color DOT imager," *Review of Scientific Instruments* **76**, 094302 (2005).

[3] L.T. Baxter and R.T. Jain, "Vascular and interstitial transport in tumors," in *Tumor Blood Supply and Metabolic Environment: Characterization and Implications for Therapy* (Gustav Fischer Verlag, Hamburg, 1990), pp. 155-164.

[4] Y. Pei, H.L. Graber, and R.L. Barbour, "Influence of systematic errors in reference states on image quality and on stability of derived information for DC optical imaging," *Applied Optics* **40**, 5755-5769 (2001).

[5] R.L. Barbour, H.L. Graber, Y. Pei, S. Zhong, and C.H. Schmitz, "Optical tomographic imaging of dynamic features of dense-scattering media," *J. Optical Society of America A* **18**, 3018-3036 (2001).

Acknowledgments

This research was supported by the National Institutes of Health (NIH) under grants 1R43CA91725-1A1, R21-HL67387, R21-DK63692, and R41-CA96102; by the U.S. Army under grant DAMD017-03-C-0018; by the New York State Department of Health; and by the Susan G. Komen Foundation under grant IMG0403022.